ADVANCED MATERIALS

DOI: 10.1002/adma.200600376

Quantum Dot Thin Layers Templated on ZnO Inverse Opals**

By *Pedro D. García*, *Álvaro Blanco*, *Alexey Shavel*, *Nikolai Gaponik*, *Alexander Eychmüller*, *Benito Rodríguez-González*, *Luis M. Liz-Marzán*, and *Cefe López**

It is well known that nanostructuring materials in a complex or ordered fashion can modify their fundamental properties. This powerful route can also combine different materials and be used to explore new properties of the resultant heterostructures, enhancing or hindering the individual properties of the constituents. In particular, by nanostructuring light-emitting materials one can modify their emission properties and tailor their response in what has revealed to be a powerful strategy to build up applications in photonics. In this way, photonic crystals (PCs)[1,2] have turned out to be a promising tool to engineer at will, or even inhibit, the emission of light. In these systems, the refractive index is modulated periodically in one, two, or three dimensions. This fact provokes the appearance of energy intervals, called photonic bandgaps (PBG), for which the propagation of light is prevented. Conveniently used, this specific property of PCs is the origin of an important number of fundamental phenomena that have been the subject of study for the last two decades.[3] Present and future photonic technologies will make use of techniques such as lithography,[4] holography,[5] direct laser writing,[6] and self-assembly[7] in order to fabricate periodically ordered nanostructures able to shape and modify fundamental optical properties of the constituent materials. Among them, structures such as artificial opals,[8] self-assembled face-centered cubic (fcc) structures of dielectric microspheres, have revealed to be a perfect playground in the field of PCs. Although as-grown, these systems do not present a complete PBG (a stopgap in all directions) and their symmetry and topology are fixed by the growth process, there is, up to now, no other method of fabrication that can provide the same large-scale fabrication, high optical quality, and versatility of processing in one package. Therefore, the combination of luminescent materials with PCs, in particular with opals, is one of the open challenges being addressed nowadays.

Light emitters such as organic dyes[9–11] and semiconductors[12–14] have been incorporated within the structure of artificial opals during the last few years. Very recently, partial inhibition and enhancement of the spontaneous emission has been shown in inverse titania opals doped with CdSe nanocrystals (NCs), matching the first (incomplete) pseudogap (pG).[15] Among the materials for this purpose, ZnO appears to be a very interesting one because of its remarkable properties as a conductor and transparency in the visible range of the spectra. Recently, high-quality ZnO inverted opals grown by chemical vapor deposition (CVD)[16] and atomic layer deposition (ALD)[17] have been reported. Furthermore, the relatively high ZnO refractive index provides enough dielectric contrast in the inverted structure to open additional pGs in the high-energy regime,[18] which have recently been used for enabling laser emission.[19] Its ample range of transparency allows ZnO to host emitters in a broad spectral range from the IR to the UV with no hindrance derived from absorption. All these reasons make ZnO an appropriate template material where quantum dots (QD) can be conformally self-assembled.

In this communication we present a large-area, high-quality, new composite material obtained by structuring, in two steps of hierarchical colloidal self-assembly, a ZnO inverted opal with colloidal CdTe nanocrystals. We also provide experimental results of the photonic effect that the original ZnO template produces on the spontaneous photoluminescence (PL) from CdTe QDs embedded in the structure. In particular, we chose the scarcely explored[20] high-energy photonic bands of the ZnO inverted opal to show that the effect produced shows up as inhibition and enhancement of the QDs emission.

Samples were prepared starting from large diameter (700 nm) polystyrene (PS) spheres in order to place the desired photonic features (high-energy gaps) matching the QD emission band (around 640 nm for a QD with diameter $d = 4$ nm). The CdTe QDs were synthesized in water following a previously described method by utilizing thioglycolic acid (TGA) as stabilizer.[21]

Figure 1 schematically depicts the method used to fabricate the composite material. Thin-film opals (Fig. 1a) were grown using the vertical deposition method[22] and were then infiltrated (Fig. 1b) with ZnO following a modified CVD method[16] that allows a controlled conformal infiltration with precision within a few nanometers. The structure was then inverted (Fig. 1c) to obtain the ZnO template, eliminating the

[*] Prof. C. López, P. D. García, Dr. Á. Blanco
Instituto de Ciencia de Materiales de Madrid (CSIC)
and Unidad Asociada CSIC–U. Vigo
C/Sor Juana Inés de la Cruz 3, 28049 Madrid (Spain)
E-mail: cefe@icmm.csic.es
Dr. A. Shavel, Dr. N. Gaponik, Prof. A. Eychmüller
Physical Chemistry, TU Dresden
Bergstr. 66b, 01062 Dresden (Germany)
B. Rodríguez-González, Prof. L. M. Liz-Marzán
Departamento de Quimica Fisica
Universidade de Vigo and Unidad Asociada CSIC–U. Vigo
36310 Vigo (Spain)

[**] This work was partially funded by the Spanish Ministry of Science and Education under contract MAT2003-01237 and NAN2004-08843, the EU under contract IST-511616 NoE PhOREMOST and the EU Project STABILIGHT.

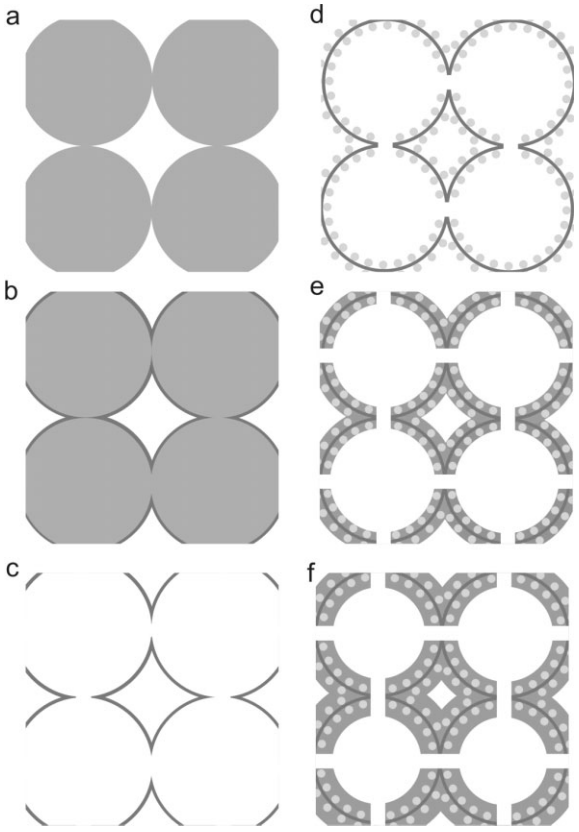

Figure 1. Schematic diagram of the method used to fabricate the composite material: a) Growth of a PS opal. b) CVD infiltration of the PS matrix with ZnO. c) Removal of the polymer matrix by calcination. d) CdTe nanocrystals conformal infiltration by dip coating. e,f) Additional ZnO infiltration by CVD.

polymer backbone by calcination. The CdTe QD infiltration of the templates (Fig. 1d) was performed as follows: ZnO inverse opals were immersed in a dilute solution containing CdTe nanocrystals and were vertically pulled with the help of a stepper motor. This leads to a precise deposition of QDs on the surface of the ZnO shells as shown schematically in Figure 1d. This process can be repeated as many times as needed. We should remark on the fact that QDs are deposited both on the inner and the outer ZnO surfaces. The inner growth is possible because the spherical air cavities are connected by windows produced at the contact points between the original spheres, which remain open after calcination. The size of these windows depends on the degree of sintering and the material used, in this case ZnO, but typically they are around 10 % of the diameter (70 nm in our case). This interior growth is possible while these windows remain open. Once the desired amount of QDs is assembled, a thin layer of ZnO can be regrown to enclose them (Fig. 1e). Additional ZnO infiltrations can be subsequently performed to obtain the desired photonic effects in the final composite (Fig. 1f).

Transmission electron microscopy (TEM; Fig. 2) and optical spectroscopy (Fig. 3) were performed to characterize the sample in addition to routine scanning electron microscopy. TEM and high-resolution TEM (HRTEM) images clearly show the fcc structure of the composite and, upon increasing the magnification, the ZnO grain size. Further increases in magnification enables observation of the atomic planes of the crystalline ZnO. The reflectance shows two peaks and transmittance shows two dips related to the first and the second pGs in the ΓL direction. For the sphere diameters investigated here, the PL emission band overlaps with the second pG of the ZnO photonic matrix.

The infiltration of the photonic template with QDs has only a small effect on the refractive index distribution, and hence on the photonic properties of the structure. The optical prop-

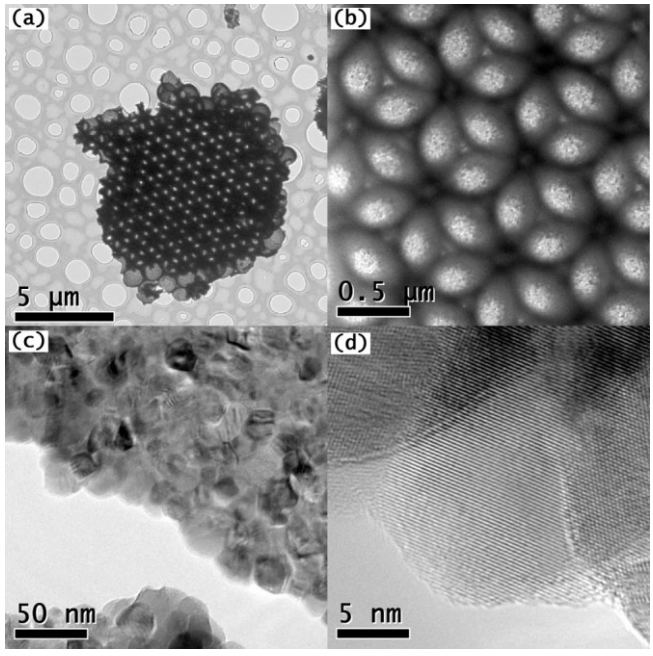

Figure 2. TEM images at different magnifications show the fcc lattice giving rise to a,b) the photonic structure, c) the ZnO nanocrystals structure, and d) the atomic lattice. The average diameter of ZnO grains can be estimated as 30 nm.

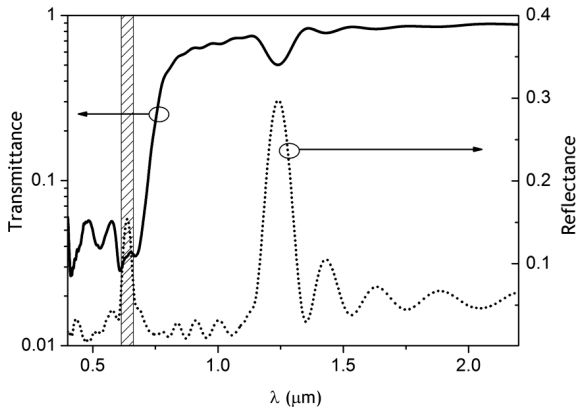

Figure 3. Reflectance and transmittance of a ZnO inverted opal. First- and second-order pGs in the ΓL direction are evident. The PL band from the QDs is represented by the dashed area.

ADVANCED MATERIALS

erties are so sensitive to these minor changes that they can be used to monitor the process with high precision by measuring the shift of the photonic features. Figure 4 shows the specular reflectance, along the ΓL direction (normal to the (111) planes) versus energy in reduced units (a/λ, where a is the lattice parameter and λ is the wavelength in vacuum) for a ZnO inverse opal after several immersions in the QD solution. The maxima in reflectance correspond to the high-energy pG that shifts to lower energies after every coating step. By a sequence of several immersions it is possible to fill the ZnO template with fine control over the filling fraction, thus tuning the photonic bands to the desired specifications for optimal performance. It is important to point out that this spectral displacement depends on the concentration of the QD solution employed. In order to study how the QD are deposited on the surface of the ZnO shells we modeled this process assuming that in each immersion a thin homogeneous layer of CdTe conformal to the ZnO shells is grown. We have calculated[23] the position of the mentioned photonic feature (high-energy pG) as a function of the CdTe layer thickness and compared the calculated results with the experimental spectral positions. In Figure 4b, experimental and theoretical results are plotted together showing a good agreement for a 0.5 ± 0.1 nm CdTe layer thickness on either side of the ZnO shell per immersion for this particular dip-coating condition. The final thickness after five immersions, 2.5 nm, is that of a close-packed monolayer.[24] The actual surface on which QDs assemble is, however, extremely rough at the nanometer scale (Fig. 2) and, accordingly, the QDs are not close packed. Nevertheless, the surface can be considered flat and smooth as far as the optical properties in the visible range of the spectra are concerned, because ZnO grains (typically 30 nm) are much smaller than the wavelengths involved (around 600 nm), which, in the case of dielectrics, can be considered negligible.

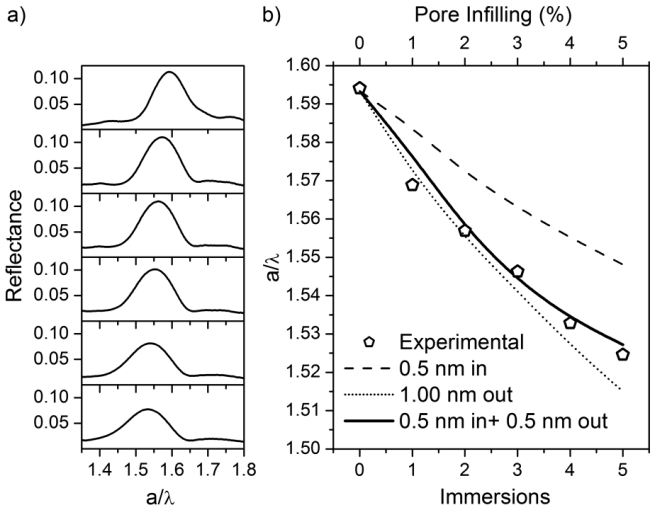

Figure 4. a) Spectral displacement of the second-order Bragg peak as a consequence of the QD infiltration. b) Open symbols represent the experimental displacement of the reflectance peak associated with the pG while the solid line represents the evolution of the pG assuming a CdTe thin layer deposition of 0.5 nm (on either side) per immersion.

We have focused our study of the photonic properties of the new composite material on the high-energy regime ($a/\lambda > 1$) where interesting phenomena like slow light or anomalous refraction can take effect and where a full PBG can emerge. Besides, in this spectral range, as opposed to the low-energy regime (first stopgap), the interplay between light and PBG environments has remained relatively unexplored. The reason for this is that very high quality samples are needed since, in this regime, the wavelengths involved are smaller than the lattice parameter. Therefore, the lattice is explored on a very short range scale where the imperfections are exacerbated. This makes this energy range particularly interesting to test the photonic properties of the new composite.

For this purpose, we have used a band-engineering strategy,[25,26] designing composites with given photonic properties by means of accurate infiltrations. A careful balance of the QD infiltration and the posterior ZnO coverage provides a means to accurately match the luminescence to the photonic gaps. In Figure 5 we show the evolution of the relevant photonic bands for the ZnO/CdTe composite as the additional ZnO layer is increased (following the scheme in Fig. 1f). The open circles represent photonic bands to which light can not couple because of symmetry restrictions and the solid lines represent the bands that determine the gap.[27] The dashed area represents the energy interval where QD emission takes place and the shaded area is the effective gap. By varying the degree of infiltration it is possible to tune this pG (see that shaded areas shift with infiltration) sweeping across the whole

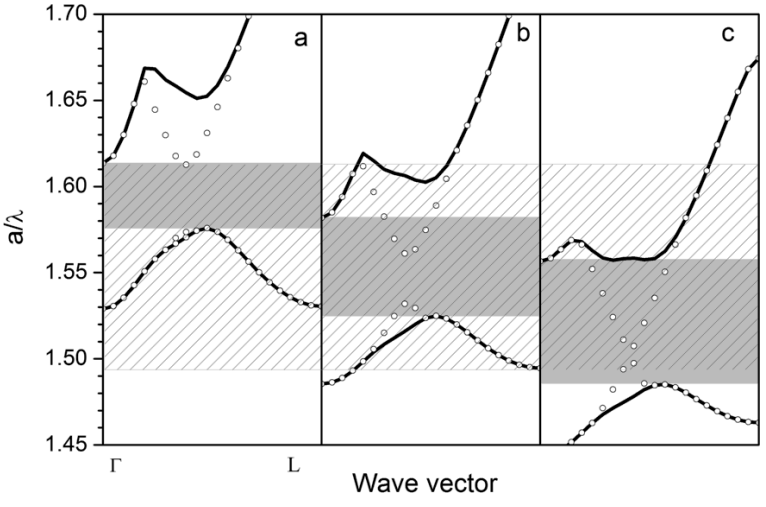

Figure 5. Band structure of QD-containing ZnO inverse opals. a) The stage where a 1 nm layer of QDs is added to an inverse opal produced by synthesizing a 31 nm ZnO layer (55 % of the pore) on the opal and inverting. In panel (b) an extra ZnO infiltration of 3 nm is added and in (c) a further 3 nm layer is grown. The PL band from the QDs is represented by the dashed area and the effective gap by the shaded rectangles. Lines represent the allowed states while dots represent uncoupled bands.

luminescence band. In this simulation, Figure 5a depicts the bands in the case of the initial structure: a 31 nm thick ZnO shell (arising from the original opal after 6 CVD cycles and inversion) coated with a 1 nm QD layer of equivalent thickness as explained above (two dip-coating immersions). Figure 5b shows the photonic bands from a structure derived from the latter one by growing a 3 nm thick ZnO layer (a single cycle of CVD) on the inner and outer surfaces of the QD decorated shell. Finally, Figure 5c corresponds to the growth of a further 3 nm thick ZnO layer in an additional single CVD cycle. The actual properties of these structures are discussed next.

The emission properties of the composites prepared were measured and compared with those of the same sources without a pG environment. To ensure that the standard PL was free from any effects arising from the interaction of the QDs and the ZnO template we used the PL emission from a pulverized sample rather than a colloidal suspension of QDs. Grinding destroys the photonic lattice and wipes out any pG effects. This system, with no pG properties but the same QD density and material properties as the original sample, is what we shall call standard PL emission. Excitation was performed with the 457.9 nm line from a continuous Ar^+ laser. Figure 6 summarizes the results from three samples differing in the amount of ZnO added (increasing from Figure 6a to c) after the QDs were adhered to the initial template. In the upper row of plots the reflectance peak is seen to shift to lower energies and broaden as we increase the ZnO content, similar to the behavior of the calculated pG (dashed areas in the figure). In the middle row, the emission spectra from the reference (PL_R; dash–dot lines) and composites (PL_C; solid lines) are plotted. Finally, the ratio of the luminescence intensities PL_C/PL_R are plotted in the bottom row in order to explicitly show the effect.

In the stage represented by Figure 6a (which corresponds to the state of the composite schematically drawn in Fig. 1d) the gap overlaps the high-energy side of the PL spectrum. Emission in this energy interval is inhibited. The result is a modified emission profile that presents a strong suppression in the high frequencies and an enhancement of low ones compared to the standard PL.

An additional infiltration of ZnO in the composite produces a red-shift of the photonic features. Figure 6b corresponds, qualitatively, to the situation drawn in Figure 1e and the corresponding photonic bands are those calculated in Figure 5b. The gap now overlaps with the central frequencies of the PL band that are therefore inhibited. The dip in the plot of the PL ratio red-shifts as the gap does.

In Figure 6c (which corresponds to the stage drawn in Fig. 1f and to the bands in Fig. 5c) the gap overlaps with the low energies of the PL band, tuning the inhibition to this side of the peak and reinforcing the emission in the high energies. We can see how in passing from Figure 6a to Figure 6c the balance of suppression and enhancement is governed by tuning the photonic bands, which in turn is controlled by the amount of material added. We see that initially there is suppression on the high-energy side and inhibition on the low, whereas in the final stage the high energies are enhanced at the expense of the low-energy range. Among possible mechanisms for PL modifications,[28] a process of electronic energy transfer[29] could explain the effect of enhancement attending to the relatively high concentration of emitters inside the composite.

One important feature we wish to point out is that the absolute value of reflectance that is causing the enhancement/suppression of the emission is only a few percent. This might not only be caused by the fact that samples are just a few layers thick; this gap, as opposed to the well-known fundamental pG at the L point, produces small reflectivities even in infinitely thick samples. In our analysis we are discounting those bands that are present in the gap but cannot couple to incoming plane waves. In reality, these bands might be actually coupling through defects and lessening the effect. Related to that, we must remark that the high-order pG appears at $\lambda = 605$ nm, which is smaller than the original PS sphere diameter (700 nm). This implies that this pG is more sensitive to the presence of defects in the sample than the first-order pG.

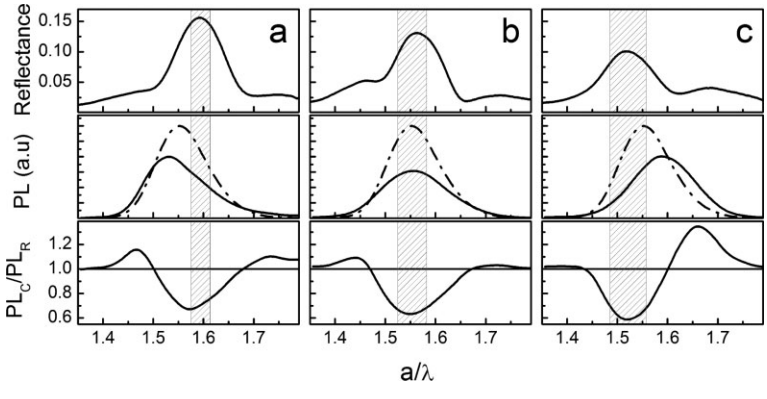

Figure 6. Each vertical panel corresponds to a different stage of additional ZnO infiltration. Upper row: the calculated spectral position of the reflectance peak in the Γ-L direction (dashed area) is shown, with the experimental reflectance, as a function of additional ZnO infiltration. The center row shows the comparison between the PL emission in the photonic matrix (PL_C, solid line) and the PL of the standard (PL_R, dashed line). Lower row: Plot of the ratio of PL_C/PL_R. Values lower than one signify inhibition whereas higher values signify enhancement of the emission.

In conclusion, we report a novel structured composite that integrates two very interesting materials, ZnO and QDs, in a photonic crystal. The fabrication is performed by an accurate infiltration in two hierarchical steps of colloidal self-assembly. The method of infiltrating a ZnO matrix with CdTe nanocrystals provides fine control over the pore-filling fraction and we prove that the infiltration of nanoparticles behaves, from a structure point of view, as a conformal thin-layer infiltration. This is to our knowledge the only way to control the infiltration of QDs. To test our composite we provide experimental results of the effect that the photonic matrix has on the spontaneous emission of the PL in the high-energy regime. We tune the CdTe QD emission to this re-

ADVANCED MATERIALS

gime of the ZnO template to profit from the wide range of infiltration produced by the large-size spheres. The presence of a high-energy pG on the spontaneous emission has been experimentally reported as an inhibition of frequencies contained in the gap and enhancement of those which are not affected by the gap. Finally, a further careful and progressive infiltration with an extra amount of ZnO has proven useful to tune this photonic effect through the PL emission spectrum. This novel procedure to build a composite from a photonic template and quantum dots in the same photonic matrix opens a route to different heterostructure materials with different types of nanoparticles.

Experimental

The opals were grown using a vertical deposition method [22] with monodisperse spheres of PS with a diameter of 700 nm. ZnO was infiltrated in the samples with a modified CVD method [15] using a organometallic precursor (1.0 M diethyl zinc solution in hexane), which allows for fine control of shell thickness (less than 8 nm per cycle). The sample was dried for 32 h at 92 °C, avoiding the melting point of the polymer backbone. At this point the samples were calcined for 24 h at 450 °C, which was reached through a ramp of 1 °C min^{-1} in order to remove PS spheres and to obtain inverted ZnO opals.

The molar ratio of Cd^{2+} ions to TGA was 1:1.3, which allowed the synthesis of high-quality NCs possessing PL quantum yields of up to 50 % without any post-preparative treatment [30]. The quantum dots infiltration was performed as follows: the photonic matrix was immersed in a dilute solution of CdTe nanocrystals in doubly distilled water with a concentration of 5.3×10^{-7} M and was vertically pulled with a step motor (Oriel Stepper-18515). A fine control over the pulling velocity (0.2 μm min^{-1}) was exerted until the sample was completely removed from the QD colloidal suspension. The sample was finally heated for 3 h at 45 °C in order to completely dry it.

Photonic band diagrams corresponding to ZnO inverted opals and the composite structure were obtained using numerical methods [23]. The refractive index of the ZnO (1.9) was measured in the spectral range used by variable angle spectroscopic ellipsometry. The specific calculations of the spectral displacement of the high-energy pG, assuming a CdTe thin-layer deposition, rapidly diverge from the experimental results when the thickness departs from 0.5 nm per immersion. This thickness is related to the initial concentration of the CdTe solution. With higher concentrations, the thickness needed to model the infiltration increases accordingly.

TEM and HRTEM images were obtained with a JEOL JEM 2010 FEG-TEM operating at an acceleration voltage of 200 kV. Samples for TEM were prepared by scratching a sample from the opal, sonicating in butyl alcohol, and depositing a drop of the dispersion on a copper grid with carbon coated holey Formvar film. The goniometer was used to tilt the sample in a suitable orientation.

Optical spectroscopy was performed with a Fourier transform IR spectrometer (Bruker IFS-66/S) by recording the normal incidence optical reflectance from visible to near-IR in regions of the samples that were 15 layers thick.

PL measurements were taken at room temperature under 457.9 nm Ar^{+} laser line excitation focused onto the back surface of the sample at non-normal incidence. The emitted light from the (111) face of the composed structure was collected with a low-aperture lens (*f*/3.5) and focused onto a spectrometer equipped with a photomultiplier tube.

Received: February 23, 2006
Final version: June 1, 2006

[1] E. Yablonovicth, *Phys. Rev. Lett.* **1987**, *58*, 2059.
[2] S. John, *Phys. Rev. Lett.* **1987**, *58*, 2486.
[3] For a recent review see C. López, *Adv. Mater.* **2003**, *15*, 1679.
[4] S. Y. Lin, J. G. Fleming, D. L. Hetherington, B. K. Smith, R. Biswas, K. M. Ho, M. Sigalas, W. Zubrzycki, S. R. Kurtz, J. Bur, *Nature* **1998**, *394*, 251.
[5] M. Campbell, D. N. Sharp, M. T. Harrison, R. G. Denning, A. J. Turberfield, *Nature* **2000**, *404*, 53.
[6] Kawata, H. B. Sun, T. Tanaka, K. Takada, *Nature* **2001**, *412*, 697.
[7] A. Blanco, E. Chomsky, S. Grabtchak, M. Ibisate, S. John, S. W. Leonard, C. López, F. Meseguer, H. Míguez, J. P. Mondia, G. A. Ozin, O. Toader, H. M. van Driel, *Nature* **2000**, *405*, 437.
[8] V. N. Astratov, *Nuovo Cimento Soc. Ital. Fis., D* **1995**, *17*, 1349.
[9] E. P. Petrov, V. N. Bogomolov, I. I. Kalosha, S. V. Gaponenko, *Phys. Rev. Lett.* **1998**, *81*, 77.
[10] M. Megens, J. E. G. J. Wijnhoven, A. Lagendijk, W. L. Vos, *Phys. Rev. A: At., Mol., Opt. Phys.* **1999**, *59*, 4727.
[11] C. López, A. Blanco, H. Míguez, F. Meseguer, *Opt. Mater.* **1999**, *13*, 187.
[12] A. Blanco, C. López, R. Mayoral, H. Míguez, F. Meseguer, A. Mifsud, J. Herrero, *Appl. Phys. Lett.* **1998**, *73*, 1781.
[13] Y. A. Vlasov, N. Yao, D. J. Norris, *Adv. Mater.* **1999**, *11*, 165.
[14] S. G. Romanov, D. N. Chigrin, C. M. Sotomayor Torres, N. Gaponik, A. Eychmüller, A. L. Rogach, *Phys. Rev. E: Stat., Nonlinear, Soft Matter Phys.* **2004**, *69*, 046 606.
[15] P. Lodahl, A. F. van Driel, I. S. Nikolaev, A. Irman, K. Overgaag, D. Vanmaekelbergh, W. L. Vos, *Nature* **2004**, *430*, 654.
[16] B. H. Juárez, P. D. García, D. Golmayo, A. Blanco, C. López, *Adv. Mater.* **2005**, *17*, 2761.
[17] M. Scharrer, X. Wu, A. Yamilov, H. Yamilov, H. Cao, R. P. H. Chang, *Appl. Phys. Lett.* **2005**, *86*, 151 113.
[18] P. D. García, C. López, *J. Appl. Phys.* **2006**, *99*, 046 103.
[19] M. Scharrer, A. Yamilov, X. Wu, H. Cao, R. P. H. Chang, *Appl. Phys. Lett.* **2006**, *88*, 201 103.
[20] L. Bechger, P. Lodahl, W. Vos, *J. Phys. Chem. B* **2005**, *109*, 9980.
[21] N. Gaponik, D. V. Talapin, A. L. Rogach, K. Hoppe, E. V. Shevchenko, A. Kornowski, A. Eychmüller, H. Weller, *J. Phys. Chem. B* **2002**, *106*, 7177.
[22] P. Jiang, J. F. Bertone, K. S. Hwang, V. L. Colvin, *Chem. Mater.* **1999**, *11*, 2131.
[23] The photonic band structure was calculated using the software MIT PHOTONIC BANDS (G. Johnson, J. Joannopoulos, *Opt. Express* **2001**, *8*, 173).
[24] The filling fraction of a monolayer of close packed spheres is $f = 0.6$, so that the effective thickness of a monolayer of particles with $d = 4$ nm is $f \times d = 2.4$ nm.
[25] F. García-Santamaría, M. Ibisate, I. Rodríguez, F. Meseguer, C. López, *Adv. Mater.* **2003**, *15*, 788.
[26] P. D. García, J. F. Galisteo-López, C. López, *Appl. Phys. Lett.* **2005**, *87*, 201 109.
[27] F. López-Tejeira, T. Ochiai, K. Sakoda, J. Sánchez-Dehesa, *Phys. Rev. B: Condens. Matter Mater. Phys.* **2003**, *68*, 115 109.
[28] M. Barth, A. Cruber, F. Cichos, *Phys. Rev. B: Condens. Matter Mater. Phys.* **2005**, *72*, 085 129.
[29] C. R. Kagan, C. B. Murray, M. Nirmal, M. G. Bawendi, *Phys. Rev. Lett.* **1996**, *76*, 1517.
[30] A. Shavel, *Ph.D. Thesis*, University of Hamburg, Germany **2005**.

